Los Alamos
National Laboratory

Tech−memo
LANSCE Division
Group LANSCE−1

To/MS: Distribution
From/MS: Frank Krawczyk
Phone/FAX: 7−1958/5−2904
Symbol: LANSCE−1:01−001
Date: 1/10/01
E−mail: fkrawczyk@lanl.gov

Subject: Status of AAA Spoke Cavity Design Simulations

This memorandum gives the status of the design simulations for a 2−gap spoke resonator at β_g=0.175. An overview of the design development as well as the final choice in geometry are presented. In addition some information is provided on the interaction between the cavity and attachments, like couplers, pick−ups etc. This status report also lists some open issues that we are aware of at this time.

General Requirements for Cavity and Coupler

A low−β superconducting cavity design for testing with beam on the LEDA accelerator is underway. The geometry requirements are given by the beam parameters at the end of the LEDA−RFQ. These require a frequency of 350 MHz (the frequency of the LEDA RFQ) and a structure length compatible with a particle velocity around β=0.12 (the beam energy at the end of the RFQ is 6.7 MeV.) To reduce the challenge given by the low particle velocity, a short 2−gap structure is proposed. The high efficiency (given by the transit time factor) of such a structure allows the use of a longer (e.g. β_g=0.175) cavity with more volume and thus lower peak surface fields. At these low beam velocities elliptical cavities are out of the question. An interesting alternative is a spoke resonator. The good rf−properties of such structures have been demonstrated in recent years e.g. at ANL. The advantages of spoke resonators include a high mechanical stability, their size (only half the diameter of an elliptical cavity at the same frequency) and their strong magnetic coupling that removes the requirement of large beam aperture for the purpose of good gap−to−gap coupling. It has been demonstrated that peak electric and magnetic fields comparable or better than for the APT β=0.64 cavities [1] can be obtained.

The beam aperture of a spoke resonator should be chosen as small as permitted by the beam−dynamics. A beam aperture sufficient for power coupling through the iris would have a very low transit time factor and too high peak electric fields. Thus the power needs to be coupled into the cavity at the outer cavity wall. The nature of the field pattern of the accelerating mode thus requires a magnetic coupling of rf−power by a loop coupler whose design will not be discussed here in detail. Nevertheless, this has significant implications for the design of the cavity. The coupler port does change the effective cavity volume more significantly than a beam−pipe coupler for an elliptical cavity. Thus its presence has to be regarded for the selection of the cavity dimensions during the design (for the correct frequency.)

General Optimization Strategy

The start of the optimization procedure uses a cylindrical cavity with a radius of approximately a quarter of the wavelength with a cylindrical spoke across its center (see Figure 1.) This sets the frequency close to the design frequency. The conventions in Figure 1 define the geometric β (β_g) and the overall length of the cavity L_{cav}=2/3 $\beta_g\,\lambda$.

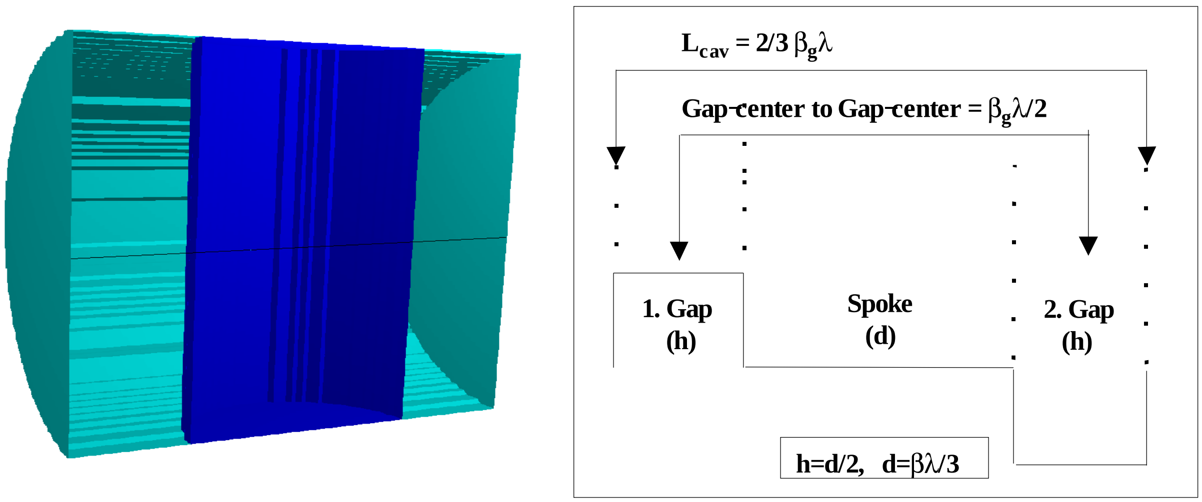

Figure 1: A simple pillbox is the starting point for optimization. The left part shows the 3D geometry, the right part shows the nominal gap−dimensions (along the black line added to the left picture) and the convention that defines the geometric β of the structure.

In Figure 2 the electric and magnetic field pattern for a generic cavity are shown. This indicates that peak electric fields can be lowered by optimizing the aperture region of the spoke and the peak magnetic fields can be lowered by optimizing the base of the spoke, where it meets the outer cavity wall. These optimizations can be done almost independently.

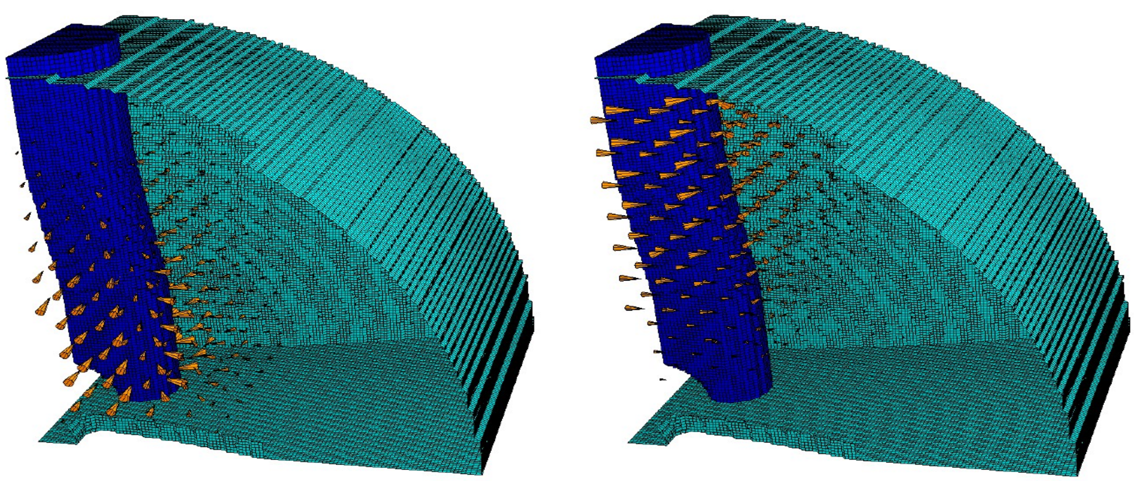

Figure 2: The left plot shows the electric field of the accelerating mode in a 2−gap spoke resonator. The right plot shows the corresponding magnetic field. The field amplitude and direction is indicated by the cones in the plot. The blue material represents a spoke, while the gray material represents the outer rf−surface of the cavity body. The electric and magnetic fields are concentrated around separate parts of the spoke geometry. This allows a fairly independent optimization of base and aperture region of the spoke.

During the optimization it turned out that also the shape of the endwall influences the highest surface magnetic field. Two different endwall geometries have been considered during the design process. One endwall shape is based on the recent ANL design [2] for the RIA project. This is a dish−shaped end−wall. The second shape is a re−entrant shape that has previously been proposed e.g. by Jean Delayen [3]. Spoke resonators of both shapes are shown in Figure 3.

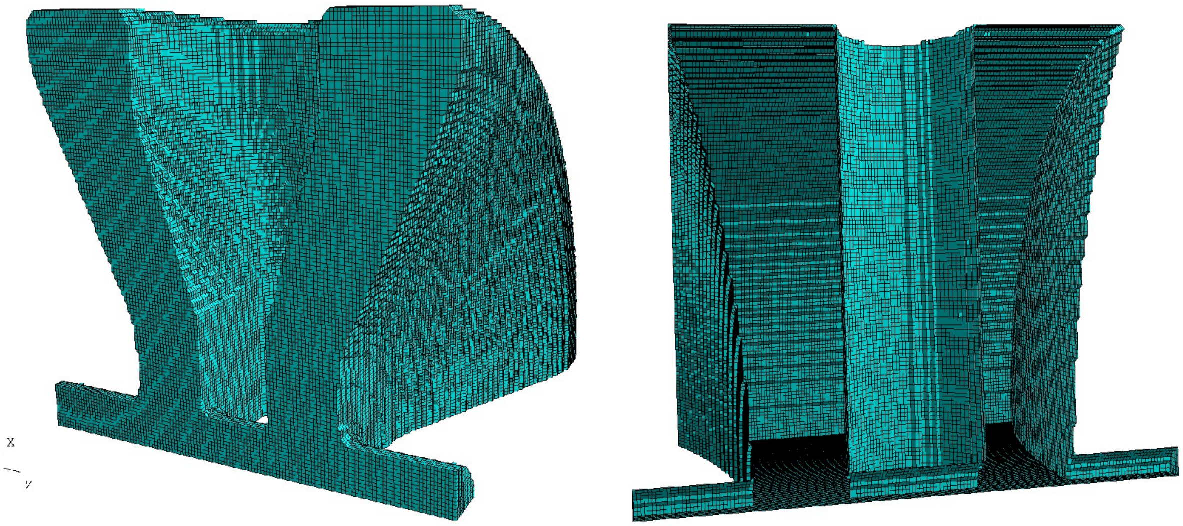

Figure 3: Two different endwall geometries (left: re−entrant, right: dish−shaped) have been considered, based on previous work on spoke resonators.

Electromagnetic Design Tools

Compared to the design work for elliptical cavities there are some challenges for designing a spoke structure. A spoke resonator is a fully three−dimensional structure. This increases the numerical effort significantly. We used MAFIA [4] as the primary electromagnetic simulation tool. Due to the complexity, comparisons have been run with other 3D tools also (MICAV, HFSS, MWS, Analyst). During the first optimization of the spoke geometry a quarter of a spoke resonator has been simulated using approximately 2 million elements. The simulation time was 3−4 cpu−hours on a SUN SPARC−2 with a 300 MHz processor. Final simulations with optimized geometries for accurate peak surface fields and frequency have been run with 6 million elements and 30 hours of cpu−time on the same workstation. The need for this huge number of elements arises form the requirement to model smooth surfaces at the locations where electric and magnetic fields peak. MAFIA by default does not necessarily have a smooth surface representation. We still preferred MAFIA due to its wider range of post−processing capabilities. Under certain conditions a choice of an inhomogenous meshing in MAFIA can still give the needed surface description quality (See Figure 4). Non−smooth surfaces in general overestimate peak surface fields.

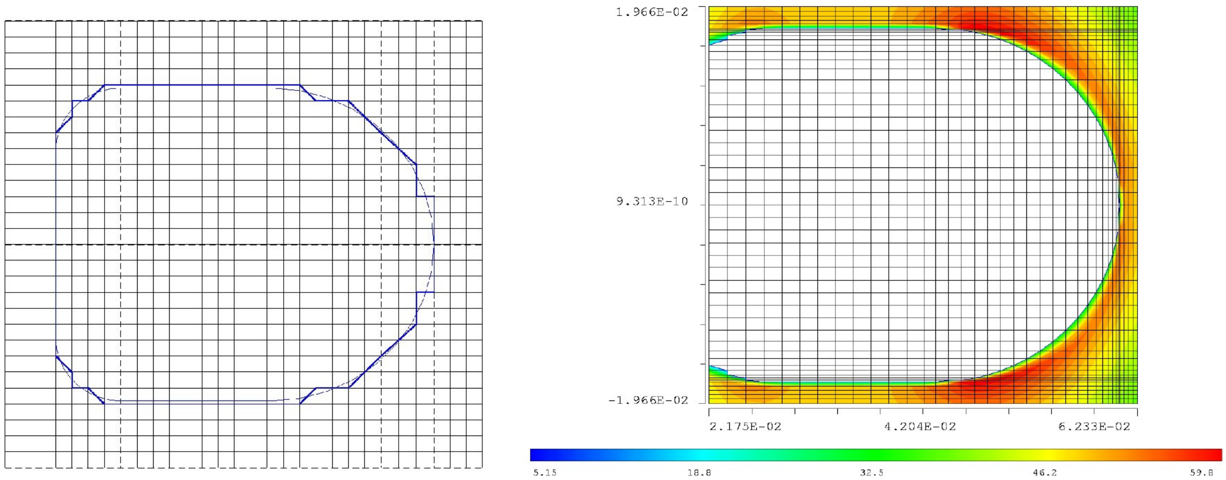

Figure 4: These two plots show a cross−section of part of a spoke in a symmetry plane in the high electric field region. A homogenous meshing (left) in MAFIA produces non−smooth curved surfaces, which leads to an overestimation of peak surface fields. A non−homogenous meshing (right, with peak electric field distribution) is required for reliable peak surface field values.

Optimization

The parameter space for optimizing a spoke resonator is much larger than for elliptical cavities. The major parameters used during the design are: cavity diameter, endwall shape, spoke−base shape and size, spoke−aperture shape and size, transition region between spoke−base and spoke−aperture. The cavity diameter was used to set the cavity frequency, while all other were used to minimize peak surface fields and maximize the transit time factor of the structure. Other considerations were mechanical stability of the structure and manufacturability. This work was significantly simplified by the possibility to interchange geometries between standard CAD and structural modeling software and MAFIA. The design of such a structure for the very low β at the end of the RFQ poses some additional challenges. Due to the short length of the cavity the available volume to increase spoke dimensions is limited. Also, due to the short focussing period the potential to lengthen the cavity for optimizing the endwalls, is limited.

The main emphasis for the optimization is to find a spoke resonator with proper length at 350 MHz (for a π−mode like accelerating field) with the lowest reasonably achievable peak surface fields (electric and magnetic.) For the base of the spoke (to minimize peak magnetic fields and thus surface currents) the shape of the cross−section and the overall diameter have been varied. The optimization for the aperture region (to minimize peak electric fields) included choosing the shape of the spoke cross−section in this region, the thickness of the spoke in beam−direction and the width of the spoke normal to the beam−direction.

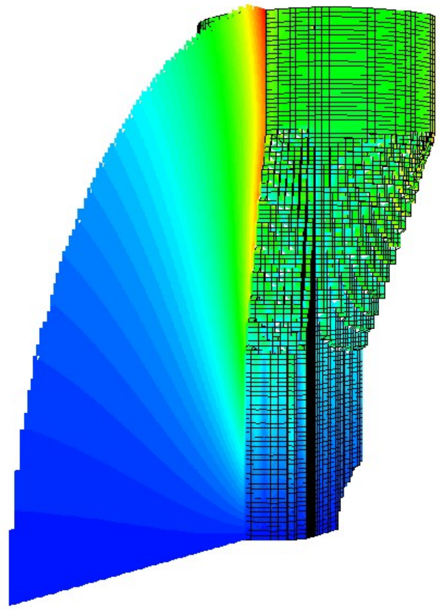

Figure 5: This plot shows a projection of the magnetic field onto a spoke surface. The surface field is fairly homogenous around the spoke circumference. Also the magnetic flux through a symmetry plane of the cavity is shown. Blue denotes the lowest and red the highest flux density in the projection.

For the base optimization cylindrical and elliptical cross−sections of the spoke have been investigated. As a result elliptical cross−sections have been ruled out as they exhibit a strongly inhomogenous distribution of surface magnetic fields with higher peaks than cylindrical spokes with a more homogenous surface field distribution (see Figure 5.)

The peak magnetic field decreases with increasing diameter of the cylindrical spoke shape. This can easily be understood considering that the increase in surface area locally decreases the surface magnetic flux density for a given total flux. The increase is limited by the interaction with the cavity endwall. If the spoke surface is too close to the endwall, the cross−section for the flux (the area between spoke and endwall) is reduced and the peak surface field will increase again (Figure 6).

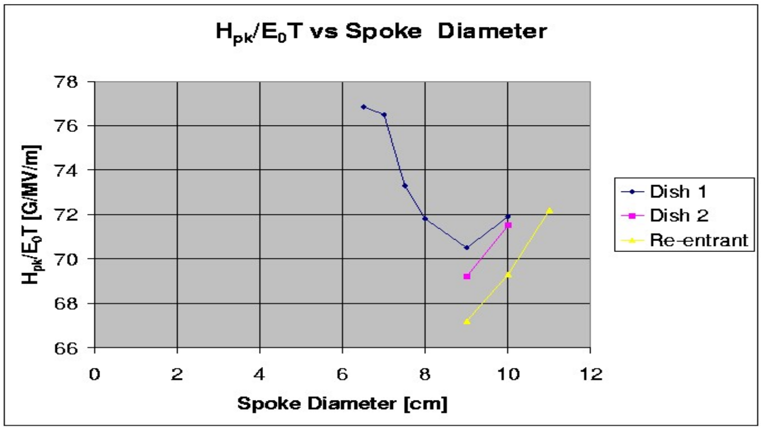

Figure 6: The graph shows the peak magnetic to accelerating field ratio for various spoke−base diameters. When the spoke−base gets too close to the endwall the peak field increases again. The results are shown for 3 different endwalls, one re−entrant and 2 dish shaped walls. Dish 1 and Dish 2 refers to two cavities with dish−shaped endwalls with identical dish−radius (50.8 cm) but different lengths (20 and 22 cm) of the outer cavity cylinders.

For the optimization of the aperture region of the spoke cylindrical, elliptical and race−track shaped cross−sections have been investigated. While for different cross−sections good peak surface electric field ratios can be obtained, the race−track cross−section had some distinctive advantages over the other solutions. First, the highest transit time factors were found for this shape. Also for manufacturability this shape has an advantage. It allows these low peak fields for a perimeter that is identical to the perimeter of the spoke at the base. This reduces production cost and effort significantly. Again, the best solution was a race−track that exhibits a fairly homogenous peak surface electric field around the periphery of the spoke (see Figure 7).

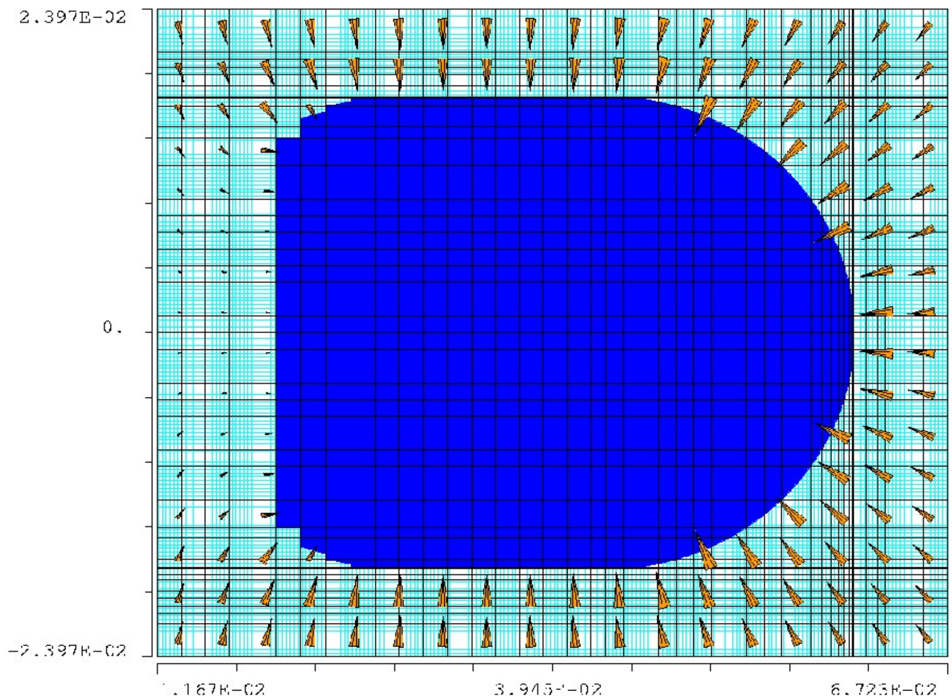

Figure 7: For the optimized spoke shape also the peak electric field is fairly homogenous around the spoke surface. This plot shows the cross−section of a part of the spoke in a symmetry plane of the cavity at the beam aperture.

Figure 6 also supports the choice of endwall we have made. While for all endwall shapes the same spoke candidate gave good peak surface fields, the best solution was a re−entrant shape that left more cross−section for the magnetic flux in the outer part of the cavity than the dish−shaped endwalls did. The shape of this re−entrant endwall was chosen to give a reasonable endwall−spoke gap over the full radial extend of the cavity.

Completion of the Cavity Model

After the selection of spoke shape and endwall shape the cavity design needs to be finalized by considering additional features that influence the final geometry of the cavity. These features are the power coupler port, a vacuum pumping port and a pick−up port. The power coupler port has to be at an angle of approximately 45 degrees off the spoke. There it will not interfere with the spoke itself, but still has sufficient magnetic field to couple to. The coupler will be a coaxial line with a loop at the center conductor tip for magnetic coupling. The size of the coupler port has been fixed by calculating the multipacting levels in coaxial lines for various geometries. These levels have been determined by scaling from the levels for the CERN LEP coupler [5], which were established by measurement. The scaling law is:

$$\mathbf{P_{MP} = P_{ori} * (f_2/f_1)^4 \, (Z_2/Z_1) \, (d_2/d_1)^4 .}$$

Figure 8 gives the lowest multipacting levels for the CERN LEP coupler and the derived levels for various coupler ports and impedances. The colors mark multipacting levels important for different scenarios of accelerator operation. The white boxes represent levels that would not be reached for any foreseen power level (12 − 149 kW). The blue boxes represent multipacting levels that would not be reached for the first spoke resonator, if the beam current does not exceed tbe minimum current of 30mA (corresponds to 12 kW). The gray boxes represent multipacting levels that would only be reached in the power coupler of the the first spoke resonator, if the beem current exceeds the minimum current of 30 mA (The maximum beam current can be up to 100 mA, which requires 40 kW input power.) The red boxes represent multipacting levels that would be reached even if the current stays below the minimum current of 30 mA.

TW /350 Mhz	CERN	AAA	AAA	AAA
MP Order	4", 75 Ω	4", 50 Ω	3", 75 Ω	3", 50 Ω
7	48 kW	32 kW	15.2 kW	10.1 kW
6	52 kW	36 kW	16.0 kW	11.4 kW
5	88 kW	60 kW	28.5 kW	19.0 kW
4	176 kW	118 kW	56.0 kW	37.3 kW
3	234 kW	152 kW	72.3 kW	48.2 kW
2	448 kW	300 kW	145.5 kW	97.0 kW
1	640 kW	428 kW	203.3 kW	135.5 kW

Figure 8: This table gives the 7 lowest one−point multipacting levels for the CERN LEP coupler and for several potential AAA coupler sizes and impedances. The AAA multipacting levels have been derived from the CERN levels by scaling.

The table shows that the 2 and 3 inch diameter couplers at 50 Ω impedance would not be an option for the β=0.175 spoke resonator. Low order multipacting bands, that are difficult to process, are already reached at low power levels. The most promising choice is the original CERN design with a 4 inch diameter and 75 Ω impedance. Based on this result a 100 mm coupler port has been added to the cavity model. Opposite to this port a second 100 mm port for vacuum pumping has also been added to the model. Their presence changes the cavity volume at a location where the magnetic field is high. This reduces the cavity frequency by 2.8 MHz. This can be compensated by reducing the cavity radius by 10.5 mm. A further correction to the frequency had to be done for a pick−up port of 1.25 inches diameter, that has been added at 45 degrees off the other side of one spoke base.

Based on all considerations in this and the previous paragraph the layout of the rf−surfaces of the spoke resonator have been determined. During the design process it was made sure that the geometry is compatible with manufacturing procedures and mechanical stability requirements.

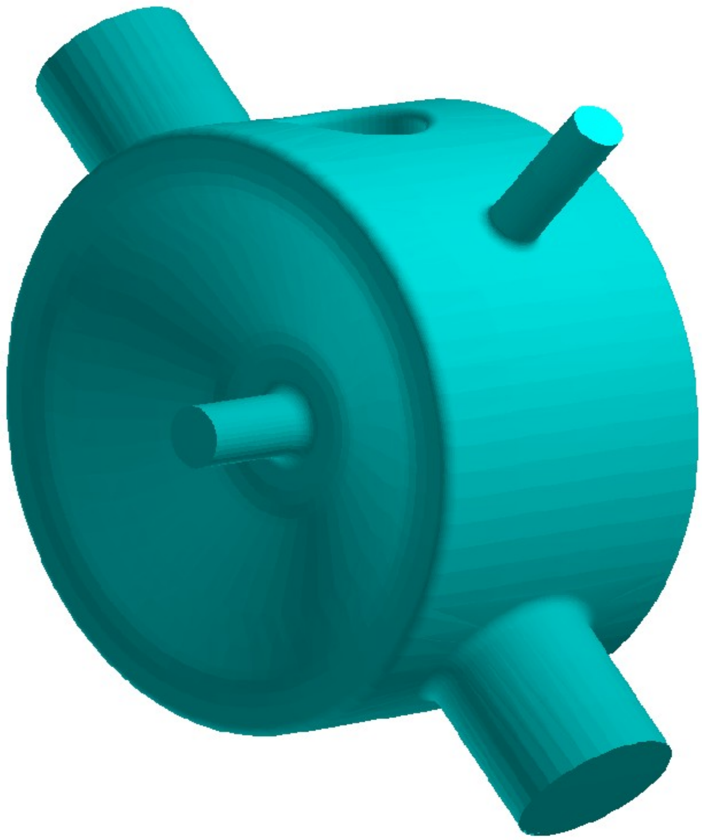

Figure 9: This plot shows full cavity model with the 100 mm ports attached. Also a pick−up port has been added.

Geometry of Choice

Figure 10 gives the dimensions that describe the optimized spoke resonator. This resonator consists of a cylindrical body with re−entrant endwalls and a spoke with a variable cross−section. The base of the spoke is cylindrical. This shape transitions into a racetrack shaped cross−section at the aperture. Table 1 gives the most important geometric dimensions of this cavity. Table 2 gives the most important rf−numbers to understand the performance of this cavity. All mechanical and structural information is provided in a different memorandum by Richard LaFave.

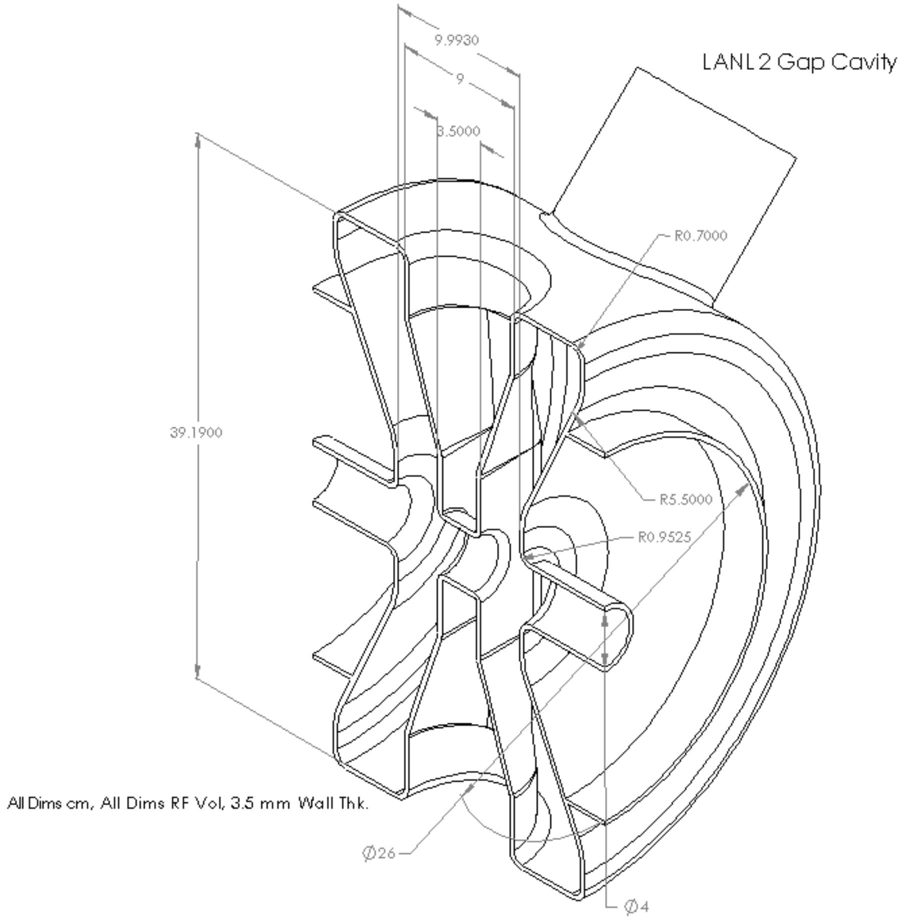

Figure 10: The basic dimensions of the rf−surfaces of the spoke resonator are provided in these figures.

Cavity Radius	19.595 cm	
Cavity Length		(Gap−to−gap)
Cavity Length		(At radius)
Spoke−base Radius	9.0 cm	
Spoke Thickness	3.5 cm	(At aperture)
Spoke Width	3.5 cm	(At aperture)
Aperture Radius	2.0 cm	
Coupler Port Radius	5.0 cm	
Vacuum Port Radius	5.0 cm	

Table 1: All dimensions of the cavity are given in centimeters. They derive from the optimization procedure described in the previous chapters.

Frequency	349.47 Mhz	
Q_0 (RT)	5628	(for 15.3 mΩ)
Q_0 (2K)	5.42E+09	(for 15.9 nΩ)
T (β_g)	0.7955	(β_g=0.175)
$T_{max}(\beta)$	0.8111	
$\beta(T_{max})$	0.2000	
E_{pk}/E_0T	< 2.84	
H_{pk}/E_0T	< 69.0 G/MV/m	

Table 2: The rf parameters in this table give the most important performance criteria of the designed resonator.

Open Issues

While we obtained a fairly complete description of the optimized spoke resonators, there are still a few open issues to be addressed. Before these issues are listed, it should be noted that this design is not the best spoke resonator available, but the best we were able to derive in the given time constraint. Since the performance data are very good, we believe that there is not enough to gain by further optimization.

The first issue that needs to be addressed further is the accuracy of the cavity frequency. The experiment in the LEDA tunnel requires a cavity that resonates very close to 350 MHz. This constraint is given by the small bandwidth of the 350 MHz klystron oscillator. The frequency derived so far is not close enough to that requirement. To fine−tune further also the magnetic loop coupler has to be added to the model. Different from a coaxial coupler on the beam−pipe its presence will noticeably influence the cavity frequency. The influence of the loop is even more complex, if one considers the fact that for different beam currents different external Qs have to be set. This is achieved by changing the orientation of the loop. Each position of the loop will give a different external Q and frequency of the cavity−coupler system. The frequency dependency on the loop orientation needs to be determined and the cavity needs to be retuned each time the external Q is changed.

It should also be noted that the design described here represents the rf−surfaces as they need to be at the operating temperature of 2 or 4 K. The room−temperature frequency (without the coupler loop present) still has to be determined. Related to this topic, also the tuning sensitivity and the total tuning range of the cavity need to be determined. Some preliminary results are reported in the structural analysis memorandum by Richard LaFave [6].

So far not much experience exists on the multipacting behavior of spoke resonators.

Threedimensional modeling with multipacting software is still in its infancy. We need to investigate if there is a good potential to determine multipacting barriers by modeling or if we have to determine during testing if multipacting barriers exist and if they can be processed.

A final remark goes to quality control. The complex nature of these cavity makes it desirable to cross−check the MAFIA results by other codes. Recently there are a few promising developments in 3D electromagnetic modeling software. We have access to some of these codes and will try to confirm as many characteristics of the cavity by using some of these alternate tools.

References

[1] Frank Krawczyk et al, "Superconducting Cavities for the APT Accelerator", Proceeding of the 1997 Particle Accelerator Conference, Vancouver (1997)

[2] Ken Shepard et al., "Prototype 350 MHz Niobium Spoke−Loaded Cavities", Proceedings of the 1999 Particle Accelerator Conference, New York City (1999)

{3} Jean Delayen, "Application of RF Superconductors to Linacs for High−Brightness Proton Beams", NIM B40/41 (1989) 892−895

[4] MAFIA Version 4.0 User Manual, published by CST GmbH, Darmstadt, Germany

[5] Joachim Tuckmantel et al., "Improvements to Power Couplers for the LEP2 Superconducting Vacities", Proceedings of the 1995 Particle Accelerator Conference, Dallas, (1995)

[6] Richard LaFave, Tech Memo LANSCE−1:01−002 (2001)

Distribution:

C. Allen, LANSCE−1, MS H817
E. Arthur, AAAPDO, MS H816
B. Baillie, LANSCE−1, MS H817
D. Barlow, LANSCE−1, MS H817
C. Bathke, TSA−3, MS F607
D. Bennett, ESS, MS H816
D. Bruhn, LANSCE−1, MS H817
M. Cappiello, AAA−FT, MS H817
K. C. Chan, AAA−FT, MS H816
K. Cummings, LANSCE−5, MS H827
R. Garnett, LANSCE−1, MS H817
R. Gentzlinger, ESA−DE, MS H821
D. Gilpatrick, LANSCE−1, MS H817
H. Haagenstad, LANSCE−1, MS H817
W. B. Haynes, LANSCE−9, MS H851
A. Jason, LANSCE−1, MS H817
P. Kelley, LANSCE−1, MS H817
F. Krawczyk, LANSCE−1, MS H817
J. Kuzminski, GAT, MS H816
R. LaFave, LANSCE−1, MS H817
G. Lawrence, AAA −1, MS H817
J. Ledford, LANSCE−1, MS H817
P. Leslie, LANSCE−1, MS H817
P. Lisowski, LANSCE−DO, MS H845
M. Lynch, LANSCE−5, MS H827
W. Lysenko, LANSCE−1, MS H817
M. Madrid, AAA−FT, MS H816
F. Martinez, LANSCE−1, MS H817
J. McGill, GAT, MS H816
J. Mitchell, LANSCE−1, MS H817
D. I. Montoya, ESA−DE, MS H821
D. R. Montoya, LANSCE−1, MS H817
A. Naranjo, LANSCE−1, MS H817
J. O'Hara, Honeywell, MS H817
N. Patterson, LANSCE−1, MS H817
D. Rees, LANSCE−5, MS H827
A. Regan, LANSCE−5, MS H827
A. Rendon, LANSCE−1, MS H817
P. Roybal, TechSource, MS H817
R. Roybal, LANSCE−1, MS H817
L. Rybarcyk, LANSCE−1, MS H817
R. Ryne, LANSCE−1, MS H817
J. D. Schneider, AAA−FT, MS H816
S. Schriber, LANSCE−1, MS H817
A. Shapiro, LANSCE−1, MS H817
R. Sheffield, AAA−FT, MS H816
E. Schmierer, ESA−DE, MS H817
F. Sigler, LANSCE−1, MS H817
H. V. Smith, AAA−FT, MS H816
G. Spalek, GAT, MS C341
J. Szalczinger, Comforce, MS H817
M. Thuot, LANSCE−8, MS H820
J. Tooker, GAT, MS H816
R. Valdiviez, LANSCE−1, MS H817
T. Wangler, LANSCE−1, MS H817
J. Waynert, ESA−EPE, MS J580
A. Wright, Butler, MS H817
R. Wood, LANSCE−1, MS H817
T. Tajima, LANSCE−1, MS H817
AAA−FT Project Office, MS H816
LANSCE−1 Reading File, MS H817